Archived at the Flinders Academic Commons

http://dspace.flinders.edu.au/dspace/

Rotational distributions following van der Waals molecule dissociation: Comparison between experiment and theory for benzene–Ar

Rebecca K. Sampson and Susan M. Bellm
School of Chemistry, Physics and Earth Sciences, Flinders University, GPO Box 2100, Adelaide, South Australia 5001, Australia

Anthony J. McCaffery
Department of Chemistry, University of Sussex, Brighton BN19QJ, United Kingdom

Warren D. Lawrance[a]
School of Chemistry, Physics and Earth Sciences, Flinders University, GPO Box 2100, Adelaide, South Australia 5001, Australia

The translational energy release distribution for dissociation of benzene–Ar has been measured and, in combination with the 6_1^0 rotational contour of the benzene product observed in emission, used to determine the rotational J,K distribution of 0^0 benzene products formed during dissociation from $\overline{6^1}$. Significant angular momentum is transferred to benzene on dissociation. The 0^0 rotational distribution peaks at $J=31$ and is skewed to low K: $J_{average}=27$, $|K|_{average}=10.3$. The average angle between the total angular momentum vector and the unique rotational axis is determined to be 68°. This indicates that benzene is formed tumbling about in-plane axes rather than in a frisbeelike motion, consistent with Ar "pushing off" benzene from an off-center position above or below the plane. The J distribution is very well reproduced by angular momentum model calculations based on an equivalent rotor approach [A. J. McCaffery, M. A. Osborne, R. J. Marsh, W. D. Lawrance, and E. R. Waclawik, J. Chem. Phys. **121**, 1694 (2004)], indicating that angular momentum constraints control the partitioning of energy between translation and rotation. Calculations for p-difluorobenzene–Ar suggest that the equivalent rotor model can provide a reasonable prediction of both J and K distributions in prolate (or near prolate) tops when dissociation leads to excitation about the unique, in-plane axis. Calculations for s-tetrazine–Ar require a small maximum impact parameter to reproduce the comparatively low J values seen for the s-tetrazine product. The three sets of calculations show that the maximum impact parameter is not necessarily equal to the bond length of the equivalent rotor and must be treated as a variable parameter. The success of the equivalent rotor calculations argues that angular momentum constraints control the partitioning between rotation and translation of the products. © *2005 American Institute of Physics.* [DOI: 10.1063/1.1847512]

I. INTRODUCTION

The dissociation of van der Waals molecules containing aromatic moieties often leads to significant amounts of rotational energy in the products.[1–6] The extent of product rotational excitation is, however, generally only qualitatively determined and based on, for example, broad widths to the rotational contours associated with the products.[2–6] Quantifying the rotational excitation is a necessary precursor to comparisons with theory. However, determining the distribution of population in the rotational states of the products is difficult since the small rotational constants of the molecules involved lead to congested rotational contours where individual transitions cannot be observed.

The purpose of this paper is to report experiments on benzene–Ar that overcome this limitation and to present a simple, transparent model for computing the angular momentum changes occurring in the polyatomic fragment during dissociation. The dissociation of benzene–Ar has been probed using a combination of velocity map imaging[7] (VMI) and dispersed fluorescence. It is shown that in combination these techniques constrain the possible rotational distributions of the benzene product.

An ability to determine the rotational distribution of the aromatic product leads naturally to the question of whether this distribution can be reproduced by theoretical models. Ideally one desires a simple model that encapsulates the essential physics of the dissociation and is able to reproduce the product distributions. In diatomic molecules it has been found that the efficient disposal of angular momentum is a critical factor in determining the product state rotational distributions in vibrational predissociation of van der Waals molecules.[8] It has also been shown that angular momentum constraints determine cross sections for rotational transfer (RT) as well as vibrational-rotational transfer (VRT),[9,10] electronic energy transfer,[11] and atom-diatomic molecule exchange reactions.[12–14] Simple calculations based on a "torque arm" for the process are very successful in reproducing ex-

perimental rotational distributions. Extension of this approach to the polyatomic case is quite challenging due to the fact that rotation may take place about more than one molecular axis. However, we have recently introduced a kinematic "equivalent rotor" model that allows the quantitative prediction of rotational distributions from inelastic collisions in polyatomic molecules for changes along *one* of these axes, i.e., for either *J*- or *K*-changing transitions.[15] Here we explore the use of this model to predict the *J* distribution for the benzene product in the dissociation of benzene–Ar. The calculated results are compared with the experimentally determined distribution and shown to provide an excellent fit.

The $S_1 \leftarrow S_0$ transition of benzene–Ar has been studied extensively. The 6^1_0 transition of the complex is redshifted 21 cm^{-1} from the bare benzene transition.[16,17] (Rotationally resolved high resolution spectra give the precise value as 21.018 cm^{-1}.[18]) The redshift of the complex to lower energy than the bare benzene indicates that it is more strongly bound in the excited state than in the ground state. The ionization energy of the complex is 74 383±2 cm^{-1}, which equates to a redshift from the benzene ionization energy of 172±2 cm^{-1}.[19–22] The binding energy of the complex has recently been measured to be 314±7 cm^{-1} in S_0, i.e., 335±7 cm^{-1} in S_1.[23] Dispersed fluorescence from 6^1, which at 522 cm^{-1} lies above the dissociation threshold, was reported by Stephenson and Rice to show bands only due to 6^1.[16] However, we have recently examined dispersed fluorescence from 6^1 at improved resolution and identified emission of the benzene product in the 0^0 state.

II. EXPERIMENTAL DETAILS

The dispersed fluorescence setup has been presented in detail in previous publications of collision-induced vibrational energy transfer from this group.[24] Benzene–Ar complexes are formed in a supersonic free jet expansion of benzene in Ar and probed 10 mm downstream from the 0.8 mm diam nozzle. The complexes are excited using the frequency doubled output of a Nd:YAG pumped dye laser tuned to 38 585 cm^{-1} (vac) to excite the 6^1_0 transition.[16] Dispersed fluorescence spectra were measured using a home-built 4.2 m Czerny–Turner spectrometer. The spectrometer uses a 6″×8″ grating with 1200 grooves/mm, blazed at 1000 nm. For the experiments reported here the spectrometer was operated in 4th order with a resolution of ca 5 cm^{-1}. The fluorescence was detected using an EMI 9813QB photomultiplier tube in combination with a digital oscilloscope (Hewlett Packard 54510A, 250 MHz, 1 GSa s^{-1}). Each oscilloscope trace was downloaded to an IBM PC clone. 256 traces were averaged at each wavelength setting of the spectrometer to give time resolved dispersed fluorescence spectra. Time integrated spectra were obtained by integrating the averaged trace at each wavelength over a 500 ns window. The benzene 6^1 fluorescence lifetime is 87 ns.[25]

The experimental details for the velocity map imaging experiments have been given in previous publications.[26] A frequency doubled, pulsed, Nd:YAG pumped dye laser (pulse duration ca. 4 ns; frequency doubled line width ca. 0.4 cm^{-1}) excites the benzene–Ar complex to an initial vi-

brational level from which it subsequently dissociates. The benzene product is ionized following absorption of a second photon from the same laser pulse. Ionization occurs in the extraction region of a time-of-flight mass spectrometer operating in velocity map imaging mode.[7] Ions are detected using a microchannel plate/phosphor screen combination and imaged onto a charge-coupled device (CCD) camera connected to a computer (IBM PC clone). Images are collected as a histogram of ion count versus position. Because dissociation is slow compared with molecular rotation, the images are isotropic and reduced to intensity versus radius for analysis and conversion to intensity versus total translational energy released. The conversion from image radius to energy is done using photoelectron images for calibration.

III. RESULTS

A. Velocity map imaging

For dissociation from 6^1, the only vibrational level of the benzene product populated is 0^0. The initial energy is well defined (522 cm^{-1}),[16] the final vibrational energy is known (0 cm^{-1}), and the dissociation energy is also known (335 cm^{-1}).[23] The energy available for rotation and translation of the products is thus 187 cm^{-1}. If the translational energy distribution is known, then the rotational energy distribution is readily calculated by conservation of energy. This rotational energy distribution refers exclusively to benzene rotation since Ar is the other product.

It will be apparent from the dispersed fluorescence spectra presented in Sec. III B below that only a small fraction of the benzene–Ar dissociates within the excited state lifetime after excitation of 6^1. It is not practical to measure velocity map images of the benzene product for dissociation from 6^1 because dissociation of the cation complex, produced by sequential two photon ionization, dominates such images. For this reason we have obtained images and translational energy release (TER) distributions for dissociation from the $6^1 1^2$ level. Dissociation from $6^1 1^2$ is known to be rapid.[16] Experiments on *p*-difluorobenzene–X (X=Ar,Kr,Xe,N$_2$,C$_2$H$_2$) (Ref. 27) and benzene–C$_2$H$_2$ (Ref. 28) complexes have found that the TER distributions are independent of the initial vibrational energy in the complex, at least for initial energies below ~3500 cm^{-1}. This is illustrated in Fig. 1, which shows TER distributions for dissociation of *p*-difluorobenzene–Ar from a series of vibrational levels in the S$_1$ state spanning the range 818–3317 cm^{-1}.[27] This corresponds to a range of energies above dissociation of 451–2950 cm^{-1}. Consequently, the TER distribution for dissociation from $6^1 1^2$ is expected to be very similar to that for dissociation from 6^1.

Consistent with previous observations,[1] the TER distribution for dissociation from $6^1 1^2$ is very well fitted by a distribution of the form

$$E^{1/2} \sum_{i=1}^{2} A_i \exp(-k_i E),$$

with $A_1 = 5.82 \times 10^{-3}$, $k_1 = 6.71 \times 10^{-2}$, $A_2 = 1.82 \times 10^{-3}$, and $k_2 = 1.74 \times 10^{-2}$. This translational energy distribution is shown as a solid curve in Fig. 2. We assume that the TER
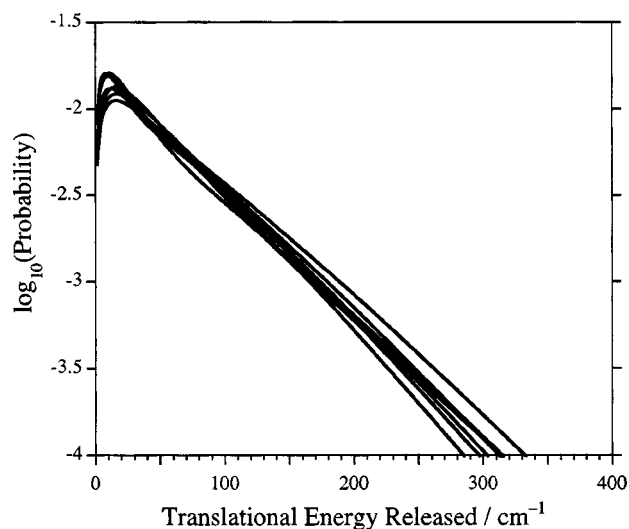
FIG. 1. A plot of TER distributions (on a logarithmic scale) for dissociation of p-difluorobenzene-Ar from a series of vibrational levels in the S_1 state spanning the range 818–3317 cm^{-1}. Data are from Ref. 27. This corresponds to a range of energies above dissociation of 451–2950 cm^{-1}. The logarithmic plot enhances differences at high energy. The distributions are very similar.

FIG. 3. Calculated 6_1^0 fluorescence band rotational contours at 5 cm^{-1} resolution for two extreme K distributions. The J,K distributions are constrained to match the experimental rotational energy distribution of Fig. 1. The lower trace has been calculated with $K=0$ for all J while the upper trace has been calculated with $K=\pm J$. The central peak is prominent for the $K=0$ distribution yet is missing for the $K=\pm J$ distribution, illustrating that the rotational contour in fluorescence can be used to ascertain information concerning the K distribution.

distribution for dissociation from $\overline{6^1}$ is the same, albeit truncated at the limit of the available energy (187 cm^{-1}). Since $0°$ is the only vibrational state that can be populated in the benzene product for dissociation from $\overline{6^1}$, the rotational energy is simply 187 cm^{-1} minus the translational energy. The rotational distribution thus obtained is shown by the dashed curve in Fig. 2.

As the benzene rotational energy is readily calculated from the usual oblate symmetric top formula

$$E(J,K) = BJ(J+1) + (C-B)K^2,$$

it is possible to calculate a distribution of population over the benzene J,K states that replicates the rotational energy distribution determined from the TER distribution. Unfortu-

nately, such a distribution is not unique as the rotational energy distribution is given in terms of two variables, J and K. The issue is how to narrow the range of possible J,K distributions.

The rotational contours of fluorescence bands from the $0°$ product are sensitive to the J,K distribution. This is illustrated in Fig. 3, which shows calculated fluorescence band rotational contours for two distributions that match the experimental rotational energy distribution of Fig. 2. The rotational constants used in the calculation are from Refs. 29–31. One of the distributions has $K=0$ for all J while the other has $K=\pm J$. It can be seen that the central peak is prominent for the $K=0$ distribution yet is missing for the $K=\pm J$ distribution. A comparison of the 6_1^0 rotational contours for various J,K distributions with the experimental contour will eliminate many of the possible J,K distributions.
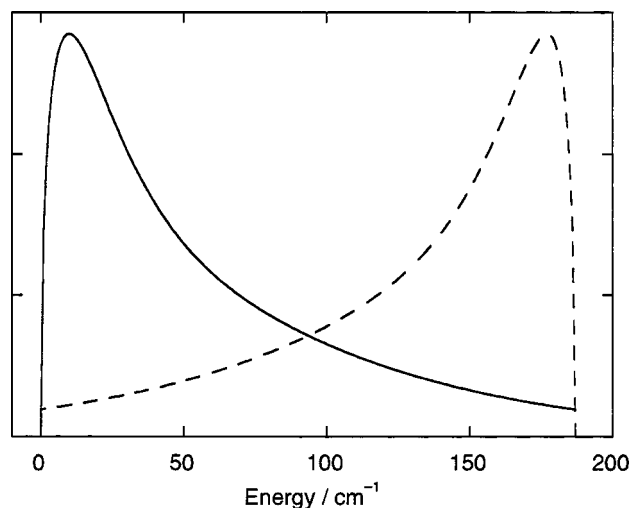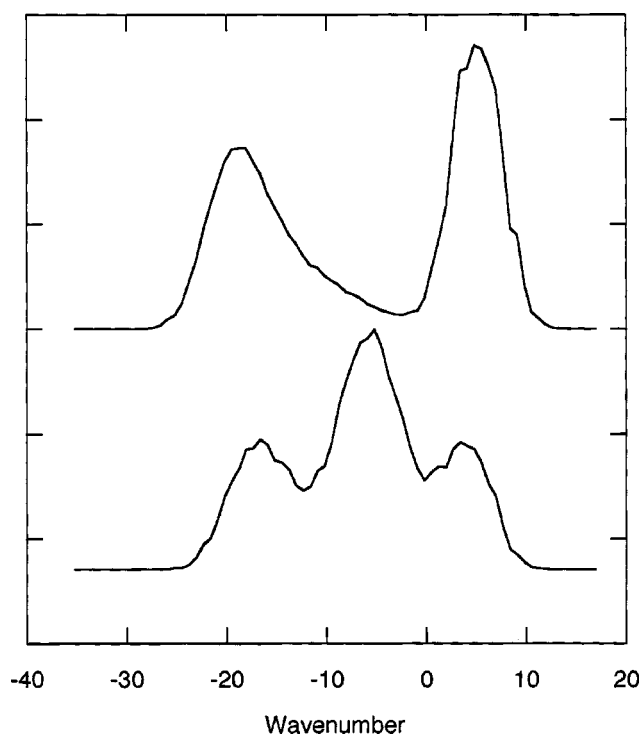

FIG. 2. Translational (solid line) and, by energy conservation, rotational (dashed line) energy distributions for products formed in dissociation from $\overline{6^1}$. The translational distribution shown is a fit to the TER distribution for dissociation from $\overline{6^1 1^2}$, which is expected to be essentially the same as that for $\overline{6^1}$ (see text).

B. Dispersed fluorescence and the 6_1^0 rotational contour

Dispersed fluorescence spectra of $\overline{6^1}$ benzene–Ar from -650 to -1800 cm^{-1} relative to the excitation position at 38 585 cm^{-1} are shown in Fig. 4 for various delay times following excitation. The spectral resolution is 5 cm^{-1}. The main growth band is 6_1^0, which is shown enlarged in Fig. 5. Stephenson and Rice reported that there was no dissociation
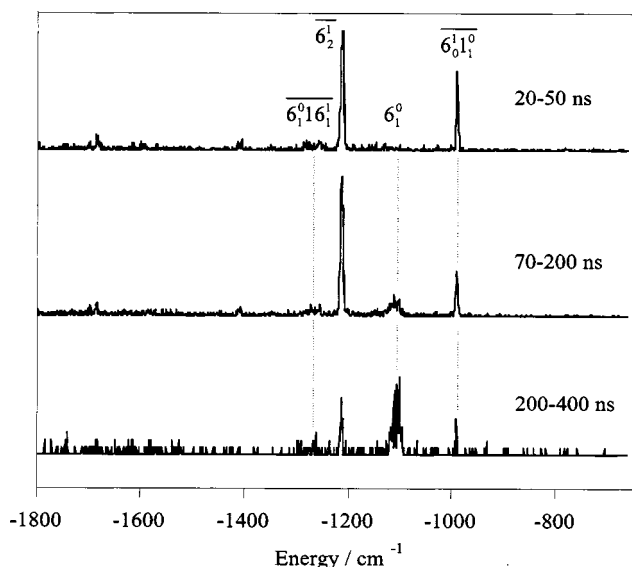
FIG. 4. Time resolved dispersed fluorescence spectra following excitation of $\overline{6^1}$. The resolution is 5 cm^{-1}. The time interval over which each spectrum has been collected is indicated on the right and corresponds to the delay from laser excitation. 6_1^0 is a prominent growth band, indicating that the complex dissociates from $\overline{6^1}$, producing 0^0 benzene. The other growth band observed is $\overline{6_1^0 16_1^1}$ which arises from population of $\overline{16^1}$ in the complex via intramolecular vibrational energy redistribution (IVR).
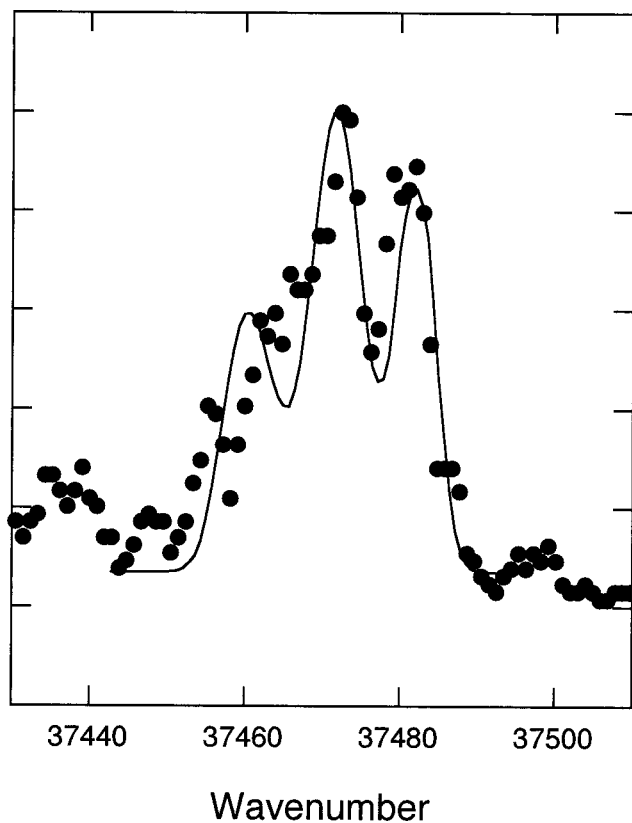

FIG. 5. The 6_1^0 band in dispersed fluorescence (5 cm^{-1} resolution) on an expanded scale. The fluorescence is integrated over a 500 ns window from the laser excitation. The circles are the experimental points, which have undergone a moving three point averaging to reduce scatter. The solid curve is a fit to this contour with the J,K distribution constrained to match the experimental rotational energy distribution shown in Fig. 1. The K distribution is calculated using form (1) (see text).

from $\overline{6^1}$.[16] Dissociation is not a significant pathway and hence would not be readily observed at the lower resolution of their study.

The 6_1^0 rotational contour is unusual when compared with a thermal contour. It is spread over $\sim$35 cm^{-1}, which requires significant population in higher J states, and shows the Q branch having significant intensity. Except at very low temperatures, the benzene thermal rotational contour shows a prominent R branch head with the Q and P branches merging and giving rise to a lower intensity "tail."[30] At low temperature the contour narrows considerably due to the loss of population in higher J,K states. The 6_1^0 contour shows that 0° is populated up to high J and that the population distribution is nonthermal.

C. Calculations of the 6_1^0 rotational contour

The VMI results provide the rotational energy distribution, but this does not provide a unique J,K distribution. The 6_1^0 rotational contour provides a means to eliminate many of the possible distributions since they will not give rise to a contour consistent with that observed experimentally. Our approach to obtaining the J,K distribution is to assume a functional form for the K distribution. For simplicity we have used functional forms involving a single variable α. Given a functional form for the K distribution, the J,K distribution can be calculated from the rotational energy distribution shown in Fig. 2 and the 6_1^0 rotational contour for this distribution calculated. This can be compared with the experimental contour and α varied to obtain a close match between the calculated and experimental contours. While this does not lead to a unique J,K distribution, the combination of the rotational energy distribution and the fluorescence rotational contour constrain the acceptable distributions.

To investigate the sensitivity of the final J,K distribution to the functional form chosen, the calculations were performed using four different functional forms. The functional forms used were

$$f(K) = \exp(-\alpha|K|), \tag{1}$$

$$f(K) = \exp\left(-\frac{K^2}{0.36\alpha^2}\right), \tag{2}$$

$$f(K) = \exp\left(-\frac{K^2}{0.36\alpha^2 J^2}\right), \tag{3}$$

$$f(K) = \exp[-\alpha(J - |K|)]. \tag{4}$$

Here $f(K)$ is the relative fraction of population in a state with rotational quantum number K.

Form (1) is an exponential decay from $K=0$. For this case $\alpha=1$ leads to a constant population in the K states prior to weighting by the rotational energy distribution. A large value of α causes the population to be heavily weighted to low K states.

Form (2) is a Gaussian distribution centered at $K=0$, with a full width at half maximum (FWHM) of α. A small value of α leads to a distribution with predominantly low K values while a large value of α leads to a uniform population

TABLE I. The K distribution parameters that provide the best fits to the experimental 6_1^0 rotational contour and the average J and K values for those distributions.

K distribution function	α	$J_{average}$	$|K|_{average}$
$f(K) = \exp(-\alpha|K|)$	0.07	27.0	10.4
$f(K) = \exp\left(-\dfrac{K^2}{0.36\alpha^2}\right)$	35	27.0	10.6
$f(K) = \exp\left(-\dfrac{K^2}{0.36\alpha^2 J^2}\right)$	1.0	26.9	10.0

of K states. [A very large value of α is equivalent to the α $=0$ case in Form (1); a very small value of α is equivalent to the large α case in Form (1).]

Form (3) is also a Gaussian distribution centered at $K=0$, but in this case the FWHM is αJ, i.e., the Gaussian width increases linearly with J. This allows the width of the K distribution to increase as the J value increases. As for Form (2), a small value of α leads to a distribution with predominantly low K values while a large value of α leads to a uniform population of K states.

Form (4) is an exponential decay similar to that of Form (1), however, in this case the distribution decays from $K=J$. A large value of α leads to a distribution with predominantly high K values while a value of zero leads to a uniform population of K states.

It can be seen that these functional forms allow the creation of K distributions that are skewed to low K, are uniform, or are skewed to high K. Figure 3 showed the contours predicted for distributions skewed to low and high J. These calculations were undertaken using forms (1) and (4) with large α. The contours are calculated for a spectral resolution of 5 cm^{-1}, which corresponds to the experimental resolution. It can be seen that the central Q branch is prominent when the K population is limited to $K=0$. It disappears entirely when the K distribution is limited to $K=\pm J$. Therefore, the relative height of the Q versus R branch is indicative of whether the K distribution is skewed to low or high K. The experimental contour is shown in Fig. 5, from which it can be seen that the Q branch is prominent, indicating that the population is skewed to low K.

Given that the 0^0 rotational distribution is skewed to low K, forms (1)–(3) are appropriate distributions to trial. α was varied for these three forms until the predicted 6_1^0 rotational contour gave a good match with the experimental contour. The calculated contour for form (1) is shown in Fig. 5 with the experimental data. Overall the fit is good, especially in view of the scatter in the data, although it does appear that the low energy edge of the contour is not as well reproduced as the remainder, suggesting that the true K distribution is more complex than allowed for by the functional forms used. Nevertheless, the distribution is reasonably approximated by these functions. The three forms give indistinguishable best fit contours at this resolution (5 cm^{-1}) and the corresponding J, K distributions are also very similar. The α values for the three distributions and the average J and K values are summarized in Table I. Figure 6 shows the J distribution that
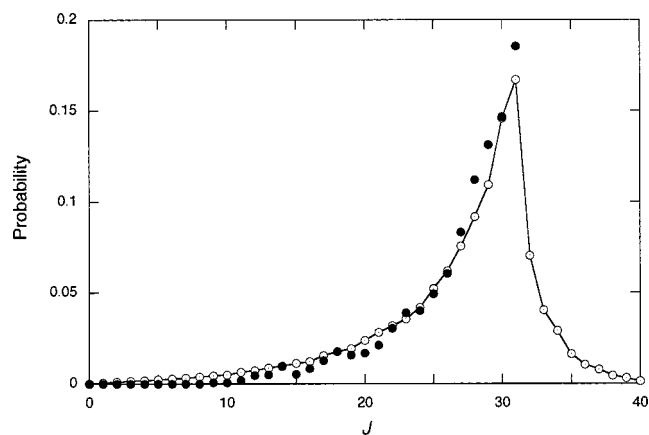

FIG. 6. Open circles show the 0^0 benzene J distribution extracted from the constrained fits to the 6_1^0 dispersed fluorescence contour. The J distribution is determined by summing over the K states for each J. Closed circles show the 0^0 benzene J distribution calculated using the equivalent rotor model (see text). The reason for the experimental distribution continuing beyond the calculated one is discussed in the text.

emerges using form (1). [The K distribution is of course given by Form (1) with the appropriate value of α.] The J distributions for forms (2) and (3) are essentially identical to this.

IV. CALCULATED J DISTRIBUTIONS

The primary act of dissociation in weakly bound complexes of *diatomic* molecules is vibration-to-rotation transfer with simultaneous breaking of the weak van der Waals (vdW) bond. This has been established using high-resolution methods from which it is evident that the process shares much in common with collision-induced vibration-rotation transfer. An adapted form of the angular momentum (AM) model of (VRT) (Ref. 8) accurately reproduces rotational distributions for vibrational predissociation (VP) in a wide range of diatomic vdW complexes.

For polyatomic vdW complexes there are practical difficulties in obtaining rotationally resolved data of the quality available for diatomics, as noted earlier. The Kelley–Bernstein model has been widely used to calculate VP rates.[32] This method, based on Rice, Ramsperger, Kassel, Marcus (RRKM) theory, is a sequential model in which dissociation occurs only after intramolecular vibrational redistribution (IVR) has populated the vdW modes with greater energy than the vdW binding energy. This approach was recently used to model VP rates in *p*-difluorobenzene-rare gas complexes.[33]

Our focus is on the subsequent dissociation step and the rotational excitation that ensues. In this section we describe an extension of the "internal collision" model of VP in vdW complexes of diatomic molecules[8] to the polyatomic case. The method utilizes the equivalent rotor model introduced as a means of calculating rotational distributions following inelastic collisions in polyatomic species.[15] In this approach J- or K-changing processes are simulated using a rigid ellipsoid, the so-called equivalent rotor. The equivalent rotor is essentially a homonuclear diatomic representation of the polyatomic. It has the same moment of inertia and major axis

length as that of the polyatomic along the inertial axis giving rise to particular J- or K-changing transitions. The model was found to successfully reproduce RT and VRT relative rate constants in glyoxal–Ne collisions, RT relative rate constants in C_2H_2–He collisions, and distributions extracted from experimental lineshapes for C_6H_6–H_2, –D_2, and –CH_4 collisions.[15] The more difficult task of predicting simultaneous J- and K-changing processes was not attempted though it was noted that experiment indicates that *either* J- or K-changing processes tend to dominate inelastic transfer in large molecules.

The model used here for VP in benzene–Ar is a direct analog of that used successfully in diatomics in which dissociation is induced by an internal collision between the molecule and weakly bound species as each executes quasi-independent vibrational motion.[8] In this process the Ar atom is ejected and vibrational excitation is converted to rotational excitation of the 0^0 level. The model is sensitive only to the energy available for transfer to rotation and translation of the products and is independent of how this is distributed within the complex prior to dissociation, i.e., the calculations are not affected by whether dissociation occurs from $\overline{6^1}$ or isoenergetic levels accessed by IVR. The outer turning point of the bond stretch vibration was found to be a significant point for vibration-to-rotation conversion in the dissociation of complexes with diatomics. In the calculations performed on C_6H_6–Ar the "bond length" b_n^{max} of the equivalent rotor was treated as an adjustable parameter in order to gain information on the point at which dissociation takes place. The calculation is based on the angular momentum method for VRT in which the overall energy constraint is set by E_{avail}, i.e., the energy of the $\overline{6^1} \rightarrow 0^0$ transition, which is the 6^1–0^0 energy gap minus the binding energy of the vdW complex.[9]

In AM model calculations there are no adjustable parameters once the value of b_n^{max} has been set. As mentioned above, this quantity will generally not be known for benzene–Ar since its value will depend on the equilibrium location of the Ar atom and the amplitude of its motion relative to the benzene ring. The calculation of the 0^0 J_f distribution is also sensitive to the value of J_i in the $\overline{6^1}$ level and computations were performed for a range of J_i values. The shape and peak J_f value were found to be quite sensitive to both b_n^{max} and J_i, although each affected the final distribution differently and so it proved possible to be quite precise regarding the optimal values of these two quantities. The calculated best-fit data are shown in Fig. 6 with the distribution extracted from the experimental data. The best values of the two parameters were $b_n^{max} = 3.7 \pm 0.1$ Å and $J_i = 8 \pm 1$. The former of these quantities is a measure of the furthest distance of the Ar atom from the center of mass of the benzene molecule at the moment of dissociation.

The fit to the experimental J distribution is very good, with both the overall shape and peak of the distribution being well reproduced. The experimental J_f probabilities continue beyond that nominally allowed by the calculated value of E_{avail} though they fall off very rapidly in probability. They originate from higher J_f states with $|K| > 0$ that are allowed

because for benzene, being an oblate symmetric top, the rotational energy decreases with increasing $|K|$. Such states were not included in our calculations.

The experimental results indicate that the dissociation leads primarily to changes in J rather than K. We noted earlier that in many experiments either J- or K-changing processes dominate. Calculations of K changes on dissociation are able to match the extracted $K_{average}$ with $b_n^{max} = 0.65$ Å. The small value of b_n^{max} is a natural consequence of the small values for K_f and indicates a restricted ability to provide torque about the K axis. The calculated K distribution rises in an exponential-like fashion, peaks at $K = 10$ and falls sharply to be zero by $K = 12$. In comparison, the three forms used to model the K distribution all fall from a maximum at $K = 0$. Higher resolution dispersed fluorescence spectra are required to give further insight into the K distribution.

The equivalent rotor AM model determines the K distribution based on a torque arm for K-changing collisions and the energy available and in consequence will not produce K distributions that peak at zero. The distributions will, however, peak at low K when b_n^{max} is restricted to small values. A small b_n^{max} for K axis changes is likely to be a common feature of dissociation from planar oblate (or near oblate) symmetric tops where the complexed atom or molecule is above the plane since the torque induced by dissociation will be primarily about the degenerate moment of inertia. In contrast, for the case of a planar prolate (or near prolate) top where the unique axis is in the molecular plane, the complexed species pushing off from the planar face can lead to rotation about the unique axis, i.e., excitation in K. In this case b_n^{max} should be large.

The calculations reproduce the experimental results with J_i tightly constrained to 8 ± 1. Is this reasonable? The rotational contour of the complex has been measured by Weber *et al.* at 130 MHz resolution.[18] There is a central, congested Q branch consisting of a number of sub-bands of lines with constant K'' and ΔK but varying J''. At lower resolution this Q branch forms an intense peak and corresponds to the spectral feature excited in our experiments. The laser excites a range of initial J states determined by the population distribution in the initial vibrational level. We do not have the resolution to see the rotational structure of the complex and hence determine the population distribution, however, our expansion conditions closely match those of Weber *et al.* and so the temperatures are expected to be similar. They find the rotational population to be described by two temperatures, 2.3 and 4.1 K. The former fits the low J while the latter fits the high J. For 2.3 K the average J value is 6 while for 4.1 K it is 8. As the authors do not give information on the relative populations at these two temperatures we cannot say what the relative weightings should be in a calculation of the average J value, but indications are that the average initial J in the excited complex is ~7. This is in excellent agreement with the J_i value required for the calculations to fit the experimental distribution.

V. DISCUSSION

The experimental results clearly show that the benzene product is formed with significant rotational excitation. The

average translational energy of the products (benzene + Ar) is 67 cm^{-1} compared with an average of 120 cm^{-1} for rotational excitation of benzene. The available data consistently point to dissociation of aromatic vdW complexes causing significant rotational excitation of the aromatic product.[1–6] The disposal of angular momentum in such systems is thus likely to provide the controlling influence on the dissociation dynamics. The success of the AM model in predicting the shape of the benzene J distribution is evidence for this.

The J, K distribution for the benzene product provides insights into the motion of benzene resulting from dissociation of the benzene–Ar complex. The fits yield $J_{average} \sim 27$ and $|K|_{average} \sim 10.3$. K is the projection of the total angular momentum onto the unique rotational axis. The angle between the total angular momentum vector and the unique rotation axis is given by

$$\cos\theta = \frac{K}{\sqrt{J(J+1)}}.$$

For $J=27$ and $|K|=10.3$, $\theta=68°$. An angle of 0° corresponds to benzene rotating in a frisbee motion, while 90° corresponds to rotation about an in-plane axis. The benzene product is thus formed with high angular momentum in a predominantly tumbling motion rather than spinning like a frisbee. This is consistent with the Ar atom being off the center of the C_6 axis when it pushes off the benzene from a position above or below the plane. The torque imparted by this motion will cause the benzene to rotate about an in-plane axis. The AM model calculations show that the maximum torque arm is longer than the distance of the H atoms from the center of the benzene ring, i.e., the Ar atom can be beyond the H atoms at dissociation. The same conclusion is reached by determining the impact parameter associated with the average J and K values extracted from our analysis of the experimental data. This extended motion of the Ar atom is consistent with the complex being above the barrier to accessing bound orbiting states prior to dissociation.[34,35]

The success of the AM model calculations in reproducing the J distribution is encouraging. It shows that the principles found to be important in determining J distributions in diatomic systems extend to polyatomics. The Kelley–Bernstein model[32] provides a means to calculate dissociation rates of vdW complexes and to understand and rationalize the behavior observed across a series of complexes.[33] It does not, however, comment on the distribution of energy within the products. The AM model offers the possibility of extending our insight into the dissociation process by providing a quantitative understanding of the partitioning between rotational and translational excitation for each final vibrational state of the product. AM model calculations predict the rotational distribution for a given final vibrational level; the translational distribution is then determined from the rotational distribution by conservation of energy. The angular momentum constraints therefore determine the partitioning between product rotation and translation, i.e., the disposal of angular momentum controls the dissociation dynamics. We note that Yoder *et al.* found a statistical model unable to reproduce the translational energy distribution observed in pyrazine–Ar dissociation.[36] In spite of its simplicity, the equivalent rotor model for AM changes shows the promise of the AM model approach for polyatomic systems.

In this context it is interesting to explore the usefulness of AM model calculations for determining the behavior in other systems. As noted earlier, there are no rotational distribution data available for comparable polyatomic systems. There are, however, more limited data available for two other systems, *p*-difluorobenzene–Ar (pDFB–Ar) (Ref. 1) and *s*-tetrazine–Ar.[4] We consider these in turn below.

For pDFB–Ar, dissociation was studied from $\overline{5}^1$. The pDFB product is produced in several vibrational states, one of which is 0^0. From the translational energy released it was determined that the average energy in rotational excitation in 0^0 is 380 cm^{-1}. The data did not provide insight into the distribution within the J,K states but it was determined that $J_{average}$ is 95 if $K=0$ states are populated and 46 for $K=J$ populated. pDFB is a near prolate symmetric top with the near-unique axis lying along the C–F bonds. Calculations of the S_0 PES for the complex[35] show the motion of Ar from the minimum above the center of the ring towards the space between the two H atoms to have the lowest barrier. Motion towards and above the F atoms has the highest barrier. It is thus likely that off-center dissociation will occur with the Ar atom towards the H side of the ring, leading to a tumbling motion about the (near) unique axis. This will produce pDFB molecules with $K \sim J$. The most likely scenario is thus that $J_{average}$ in 0^0 is ~ 46 and that $K_{average}$ is similar. The TER distribution peaks at low translational energy, showing that little pDFB product is produced with low J.

The results of AM model calculations for this system are shown in Fig. 7. Two sets of calculations have been performed, one for J changes and the other for K changes. (The calculations assume pDFB to be a prolate symmetric top.) These calculations are predictions made with no adjustment of parameters. The available energy is determined from the vibrational energies and dissociation energy, which are known.[1,37] b_n^{max} is simply calculated in each case from the rotational constants for the corresponding equivalent rotor.[15] The initial J has been set to zero. The predictions are remarkably consistent with the experimental results. J_f peaks at 54 while K_f peaks at 47, with average values of $J_{average}=47$ and $K_{average}=41$. The distributions have little intensity at low J and K, consistent with the observed translational energy release distributions peaking at low energy. Unfortunately the experimental data do not provide sufficient insight into the J and K distributions to allow a more detailed comparison. Nevertheless, it is clear that this *a priori* prediction matches the trends in the experimental data very well, indicating that the AM model has the potential for predictive capability.

The case of *s*-tetrazine–Ar is less well determined since the only data available come from the rotational contour of the $16a_1^1$ growth band in the dispersed fluorescence spectrum from $6a^1$ ($E_{vib}=703$ cm^{-1}). The contour indicates that $J_{max} \sim 25$–30, with the distribution peaking at $J=15$. Because this is a parallel band ($\Delta K=0$), no insight is provided into the K distribution. We have not performed calculations for K changes. Note, however, that *s*-tetrazine is a near oblate symmetric top, with the unique rotation axis perpendicular to the molecular plane (analogous to benzene), and consequently
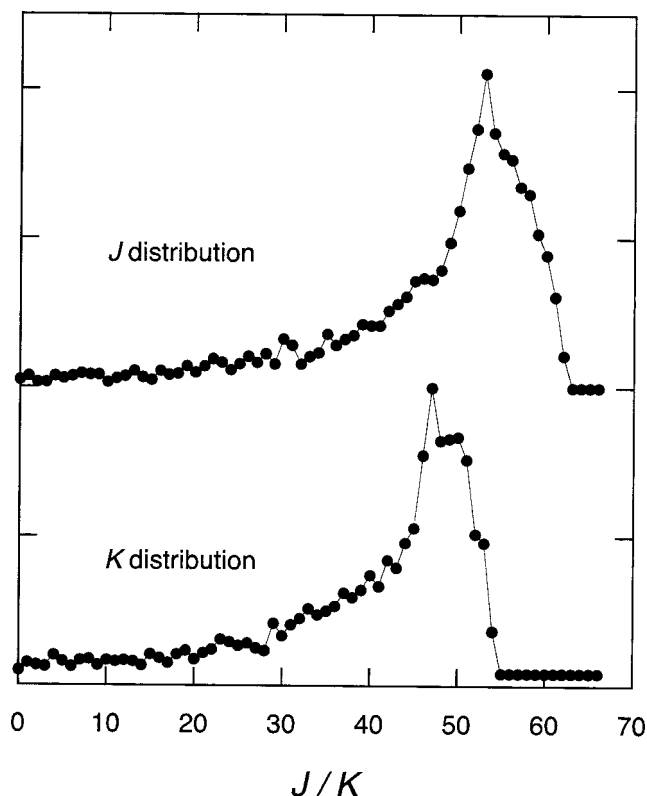
FIG. 7. Calculated J (upper) and K (lower) distributions for dissociation of pDFB–Ar. The calculations have been performed using the equivalent rotor model with parameters as described in the text.

we expect transfer to occur primarily to low K states. The s-tetrazine–Ar case is further complicated by the lack of an accurate value for the S_1 dissociation energy D_0'. Brumbaugh *et al.* determined limits of 277 cm^{-1} < D_0' < 381 cm^{-1} from the appearance of vibrational bands in the s-tetrazine product. However, they point out that the rotational excitation observed in the $16a_1^1$ rotational contour provides a means to reduce this upper limit. The maximum rotational excitation was estimated to lie in the range $J=25$–30. Brumbaugh *et al.* deduced the dissociation barrier to be < 306 cm^{-1} for J_{max} $=25$. The difficulty is that the K state population is not known and K states stack to lower energy in this molecule. Thus, if the highest J states are populated with $K=0$, there is less energy in rotation than has been used to determine this estimate, which is for $K=0$. We have taken a conservative upper limit of 330 cm^{-1}, corresponding to $J=25$, $K=15$, for the purposes of illustrative calculations.

Two sets of calculations have been performed, one with $D_0'=277$ cm^{-1} giving an available energy E_{avail} of 172 cm^{-1}, and the other with $D_0'=330$ cm^{-1} for which E_{avail} $=118$ cm^{-1}. We find that in order to obtain a J distribution peaking at 15 and extending to 25 we need (i) a modest value for b_n^{max} (1.0±0.1 Å for $E_{avail}=172$ cm^{-1}; 1.25±0.1 Å for $E_{avail}=118$ cm^{-1}) and (ii) J_i in the range 2–6. These values for b_n^{max} are smaller than the value determined for the equivalent rotor. The modest values for b_n^{max} required for s-tetrazine–Ar are in contrast to the larger values required for benzene–Ar and pDFB–Ar. Further work is needed to determine the reason for the different values of b_n^{max} required in different molecular systems. Unfortunately information is

not available concerning the initial J distribution for the s-tetrazine–Ar complex and so we are unable to compare experimental values with those required by the model calculations.

VI. CONCLUSIONS

The translational energy release distribution and the 6_1^0 rotational contour in dispersed fluorescence have been used in combination to obtain a rotational J,K distribution of 0^0 benzene products formed in the dissociation of $\overline{6^1}$ benzene–Ar. Significant angular momentum is transferred to benzene on dissociation. The 0^0 rotational distribution peaks at $J=31$ and is skewed to low K; $J_{average}=27$ and $|K|_{average}$ $=10.3$. From these values the average angle between the total angular momentum vector and the unique rotational axis was determined to be 68°. This indicates that benzene is formed tumbling predominantly about in-plane axes rather than in a frisbeelike motion. This is consistent with the Ar atom pushing off the benzene from an off-center position above or below the plane since the torque imparted by this motion will cause the benzene to rotate about an in-plane axis.

The total angular momentum distribution is very well reproduced by angular momentum model calculations based on an equivalent rotor. This indicates that angular momentum constraints control the partitioning of energy between translation and rotation. Calculations of the K distribution required a small b_n^{max} to reduce the torque imparted about the K axis. We suggest that this is likely to be a general feature of dissociation of complexes involving planar oblate tops when the complexed species is above the plane. Calculations for pDFB–Ar suggest that the equivalent rotor model provides a reasonable prediction of both J and K distributions in prolate (or near prolate) tops when dissociation leads to excitation about the unique, in-plane axis. Calculations of the s-tetrazine J distribution in dissociation of s-tetrazine–Ar require a smaller b_n^{max} than that of the equivalent rotor, illustrating that further development of the model is required for it to be used to predict distributions. Nevertheless, it appears to contain the essential elements necessary for such a description. Most desirable is a more sophisticated approach that can account for J and K changes simultaneously and provide a quantitative predictor of both J and K distributions. Angular momentum model calculations predict the rotational distribution for a given final vibrational level; the translational distribution is then determined from the rotational distribution by conservation of energy. A version of the angular momentum model that provides J,K distributions will allow calculation of the partitioning between product rotation and translation.

ACKNOWLEDGMENTS

[1] S. M. Bellm and W. D. Lawrance, J. Chem. Phys. **118**, 2581 (2003).
[2] G. Lembach and B. Brutschy, J. Phys. Chem. **100**, 19758 (1996).
[3] G. Lembach and B. Brutschy, J. Phys. Chem. A **102**, 6068 (1998).
[4] D. V. Brumbaugh, J. E. Kenny, and D. H. Levy, J. Chem. Phys. **78**, 3415 (1983).
[5] X. Zang, J. M. Smith, and J. L. Knee, J. Chem. Phys. **97**, 2843 (1992).
[6] H. Saigusa, B. E. Forch, K. T. Chen, and E. C. Lim, Chem. Phys. Lett. **101**, 6 (1983).
[7] A. T. J. B. Eppink and D. H. Parker, Rev. Sci. Instrum. **68**, 3477 (1997).
[8] A. J. McCaffery and R. J. Marsh, J. Chem. Phys. **117**, 9275 (2002).
[9] R. J. Marsh and A. J. McCaffery, J. Phys. B **36**, 1363 (2003).
[10] A. J. McCaffery and R. J. Marsh, J. Phys. Chem. A **104**, 10442 (2000).
[11] A. J. McCaffery and R. J. Marsh, J. Chem. Phys. **115**, 9771 (2001).
[12] K. Truhins, R. J. Marsh, A. J. McCaffery, and T. W. J. Whiteley, J. Chem. Phys. **112**, 5281 (2000).
[13] A. J. McCaffery, K. Truhins, and T. W. J. Whiteley, J. Phys. B **31**, 2023 (1998).
[14] R. J. Marsh, A. J. McCaffery, and M. A. Osborne, J. Phys. Chem. **107**, 9511 (2003).
[15] A. J. McCaffery, M. A. Osborne, R. J. Marsh, W. D. Lawrance, and E. R. Waclawik, J. Chem. Phys. **121**, 169 (2004).
[16] T. A. Stephenson and S. A. Rice, J. Chem. Phys. **81**, 1083 (1984).
[17] J. A. Menapace and E. R. Bernstein, J. Phys. Chem. **91**, 2533 (1987).
[18] Th. Weber, A. von Bargen, E. Riedle, and H. J. Neusser, J. Chem. Phys. **92**, 90 (1990).
[19] K. H. Fung, W. E. Henke, T. R. Hays, H. L. Selzle, and E. W. Schlag, J. Phys. Chem. **85**, 3560 (1981).
[20] L. Chewter, K. Müller-Dethlefs, and E. W. Schlag, Chem. Phys. Lett. **135**, 219 (1987).
[21] M. Schmidt, M. Mons, and J. Le Calvé, Chem. Phys. Lett. **177**, 371 (1991).
[22] H. Krause and H. J. Neusser, J. Chem. Phys. **97**, 5923 (1992).
[23] R. K. Sampson and W. D. Lawrance, Aust. J. Chem. **56**, 275 (2003).
[24] E. R. Waclawik and W. D. Lawrance, J. Chem. Phys. **102**, 2780 (1995).
[25] T. A. Stephenson and S. A. Rice, J. Chem. Phys. **81**, 1073 (1984).
[26] J. R. Gascooke and W. D. Lawrance, J. Phys. Chem. A **104**, 10328 (2000).
[27] S. M. Bellm, Ph.D. thesis, Flinders University, 2001.
[28] R. K. Sampson, Ph.D. thesis, Flinders University, 2003.
[29] E. Riedle, T. Knittel, T. Weber, and H. J. Neusser, J. Chem. Phys. **91**, 4555 (1989).
[30] J. H. Callomon, T. M. Dunn, and I. M. Mills, Philos. Trans. R. Soc. London, Ser. A London, Ser. A **259**, 499 (1966).
[31] J. Pliva and A. S. Pine, J. Mol. Spectrosc. **93**, 209 (1982).
[32] D. F. Kelley and E. R. Bernstein, J. Phys. Chem. **90**, 5164 (1986).
[33] T. Jayasekharan and C. S. Parmenter, J. Chem. Phys. **120**, 11469 (2004).
[34] S. M. Bellm, R. J. Moulds, and W. D. Lawrance, J. Chem. Phys. **115**, 10709 (2001).
[35] R. J. Moulds, M. A. Buntine, and W. D. Lawrance, J. Chem. Phys. **121**, 4635 (2004).
[36] L. M. Yoder, J. R. Barker, K. T. Lorenz, and D. W. Chandler, Chem. Phys. Lett. **302**, 602 (1999).
[37] S. M. Bellm, J. R. Gascooke, and W. D. Lawrance, Chem. Phys. Lett. **330**, 103 (2000).